Implantable electrical stimulation bioreactor with liquid crystal polymer based electrodes for enhanced bone regeneration at mandibular large defects in rabbit

Chaebin Kim[1,2¶], Hoon Joo Yang[3,4¶], Tae Hyung Cho[3], BeomSeok Lee[3], Tae Mok Gwon[1,2], Soowon Shin[1,2], In Sook Kim[3], Sung June Kim[1,2,5*&], Soon Jung Hwang[3,4,6*&]

[1] Department of Electrical and Computer Engineering, Seoul National University, Seoul, Republic of Korea

[2] Inter-University Semiconductor Research Center, Seoul National University, Seoul, Republic of Korea

[3] Dental Research Institute, School of Dentistry, Seoul National University, Seoul, Republic of Korea

[4] Orthognathic Surgery Center, Seoul National University Dental Hospital, Seoul, Republic of Korea

[5] Institute on Aging, Seoul National University, Seoul, Republic of Korea

[6] Department of Oral and Maxillofacial Surgery, School of Dentistry, Seoul National University, Seoul, Republic of Korea

* Corresponding author

E-mail: kimsj@snu.ac.kr (SJK)

E-mail: sjhwang@snu.ac.kr (SJH)

¶ These authors contributed equally to this work.

& SJK and SJH are Joint Senior Authors.

Abstract

The osseous regeneration of large bone defects is still a major clinical challenge in maxillofacial and orthopedic surgery. Our previous studies demonstrated that electrical stimulation (ES) with biphasic current pulse showed proliferative effects on bone cells and enhanced secretion of bone-forming growth factors. This study presents our new strategy to promote the regeneration of a large mandibular bone defect in rabbits, using an implantable electrical stimulation bioreactor, where liquid crystal polymer (LCP) was used for gold electrode attachment and as an outer box to maintain the defect outer space, because the removal of LCP is not needed owing to its excellent bone-binding property and mechanical properties similar to those of bone. The bioreactor was implanted into the rectangular bone defect sized 15 mm in length (anterior-posterior) and 7 mm in height at the rabbit mandibular body, which was subjected to ES with a biphasic current pulse (20 μA amplitude, 100 μs duration, 10 ms period) for one week. The effect of ES via bioreactor was compared with a sham control group and positive control group that received recombinant human bone morphogenetic protein (rhBMP)-2 (20 μg) by injection one week after the bioreactor implantation without ES. Bone regeneration was evaluated four weeks after surgery using micro-computed tomography. In the histological evaluation, there was no inflammation within bone defects and adjacent to LCP in all groups. New bone volume per tissue volume (BV/TV) in the ES and rhBMP-2 groups increased to 171% ($p < 0.001$) and 210% ($p < 0.001$), respectively, compared to that in the sham control group. The bioreactor system with ES was superior in bone mineral density (BMD) compared to rhBMP-2, while rhBMP-2 applied one week after surgery showed more enhanced osteogenesis than the bioreactor system with ES. This study showed that the ES bioreactor with LCP electrodes could enhance bone regeneration at large bone defects, where LCP can act as a mechanically resistant outer box without inflammation. Further studies on other conditions of the bioreactor will be helpful for more efficient bone regeneration at large bone defects.

Introduction

53 Regeneration of large bone defects has been a challenging issue in maxillofacial and orthopedic surgery.
54 Extensively researched strategies include tissue engineering with cells, scaffolds, growth factors, mechanical
55 environment, and biophysical stimulations (1-4). Direct implantation of precultured stem cells is a straight-
56 forward and effective method (5, 6). However, stem cell application for bone regeneration requires multiple
57 complicated procedures such as tissue harvesting, separation of stem cells, cultultivation of cell for proliferation
58 and differentiation, which are accompanied by long culture time, high cost and infection risk (7). Moreover, the
59 efficacy of stem cell transplantation is low because of low survival rate after transplantation (8). Bone
60 regeneration with osteoconductive cell-free substances such as allogenic, xenogenic or alloplastic bone grafts
61 showed low osteogenesis efficacy with long regeneration time (9, 10). Bone regeneration with a growth factor
62 such as recombinant human bone morphogenetic protein (rhBMP)-2 showed enhanced bone quantity with
63 reduced regeneration time in the clinical application (11-13). However, cell proliferation is not stimulated by
64 rhBMP-2, while numerous cells are required for bone regeneration at large bone defects. Another relevant factor
65 is biophysical stimulation under a suitable environment (14, 15).

66 Bone morphogenetic protein (BMP) is a well-known osteoinductive signaling chemokine that causes bone
67 formation by recruiting stem cells and differentiating them into bone-forming cells (16). Among the BMP family,
68 rhBMP-2 is widely used for bone tissue engineering because of its effectiveness in bone formation and its
69 commercial accessibility. Despite its efficacy, rhBMP-2 is rapidly diffused when injected *in vivo*, hence, often
70 high dose is required to obtain sufficient osteoinductive effect (17). However, high dosage of rhBMP is
71 associated with soft tissue hematoma swelling, radiculopathy, cyst-like bone formation, bone resorption, and
72 inflammation (18-22).

73 To overcome the aforementioned limitations in bone regeneration, tissue prefabrication or prelamination
74 techniques have been introduced for the regeneration of large bone defects. First, an avascular scaffold is
75 vascularized after its implantation into well-vascularized tissue for a period; then, the vascularized scaffold with
76 vessel pedicle is transferred to the tissue defects (23). Based on this regenerative concept, tissue engineering
77 components (scaffold, cells and growth factors) are implanted into an adequate anatomical site that can provide
78 regenerative microenvironments with well-vascularized tissue, and the components are cultivated within living

body tissue using intracorporeal self-regenerative function that acts as an *in vivo* bioreactor (23). However, most large bone defect sites have reduced vascularity owing to the previous operations, infection or trauma, and thus they cannot provide optimal regenerative microenvironments. Therefore, new bone tissue should be first engineered at a well vascularized ectopic site, and, then, transferred to the bone defect site with vascular pedicles in the second surgery. Instead of such uncomfortable second surgery for surgeons and patients, it is preferable that regenerative microenvironments at bone defect sites can be improved by an appropriate physical stimulation such as electrical stimulation (ES) (24, 25); thus, tissue engineering components without vascular pedicles can be directly transferred into the osseous defect site.

ES modulates osteogenic activities of the stem cells, which can sense and react to the electric field (26). ES has a positive effect on proliferation of bone cells, bone mineralization and expression of bone related growth factors and chemokine genes (27). Recently, biphasic electric current stimulation was proposed to be used in bone regeneration for the safety of ES by achieving charge balance (28). The biphasic electrical current stimulation on three dimensionally cultured mesenchymal stem cell accelerates the expression of chemokine receptors related to migration of the bone cells to the bone defect (24). In our previous report, the feasibility of intracorporeally installed electrical stimulators as a form of *in vivo* bioreactor for enhanced bone regeneration at large mandibular bone defects was demonstrated (24). However, the flexible electrodes did not have enough mechanical strength to maintain defect space against soft tissue tension after wound closure and external force during bone regeneration. Moreover, electrodes should be eliminated in the second surgery, because the electrodes used in the previous study were not integrated to the bone and may hinder bone union owing their area covering the cross-section of the defect.

Recently, liquid crystal polymer (LCP) has been used as a substrate for electrodes in neural prosthetic devices (29, 30). LCP is a biomaterial that has a mechanical strength similar to that of bone, an excellent affinity to bone and can be thermally deformed easily (31). It can be effectively applied as an outer box or a scaffold for bone regeneration with ES in the orthopedic and maxillofacial field, because it can be integrated into regenerated bone, therefore its removal is not necessary. On this basis, we developed an implantable bioreactor with LCP electrodes, where LCP can act as a mechanically resistant outer box in bone defect. The aim of the

105 present study was to evaluate the regeneration of new bone with or without ES, compared to that by rhBMP-2
106 without ES, at a large bone defect of the mandibular body in rabbits.

107

108 Materials and methods

109 Fabrication of bioreactor

110 The bioreactor consisted of an LCP outer box containing gold electrodes, an electrical stimulator with a
111 battery that produced biphasic electrical current pulses, and absorbable collagen sponges (ACSs) that were
112 located within the LCP outer box. The LCP outer box was designed to fit the rabbit mandibular bone defect and
113 its mechanical strength was sufficient to maintain the defect space necessary for bone regeneration. It was
114 composed of three walls: the buccal, lingual and bottom walls; therefore, the residual three walls (upper, mesial
115 and distal wall) in the hexahedral bone defect were covered with autogenous bone walls after mandibular bone
116 resection, from which cell migration, angiogenesis and new bone ingrowth into the defect space could occur.
117 Two patterned gold plates were embedded inside the LCP outer box to make the electric current flow across the
118 bone defect (Fig 1A-D). ACSs were placed inside the LCP for osteoconductive bone regeneration (Fig 1E). The
119 electrical stimulator, with a battery that was implanted in the submandibular area was connected with the gold
120 electrodes of the LCP outer box through the lead that was fabricated together with the electrodes (Fig 1F).

121

122 **Fig 1. Fabrication of the bioreactor and process of the animal experiment.**

123 (A) LCP film is prepared as a substrate of the bioreactor. (B) Gold electrodes are patterned on the substrate. (C)
124 Macro- and micro-holes are fabricated through the patterned film. (D) The film is deformed to be conformal to
125 the bone defect. (E) Collagen sponge is mounted in the space between the electrodes. (F) Electric stimulator is
126 connected to the extension plate. (G) Mandibular bone defect is created by osteotomy. (H) The bioreactor is

implanted to the bone defect and fixed with screws.

LCP outer box with gold electrodes

The LCP outer box was fabricated using LCP films (Vecstar, Kuraray, Tokyo, Japan) (Fig 2). The LCP outer box was made as follows. First, an LCP film was attached on a silicon wafer using a spin-coated silicone elastomer. Gold and titanium seed layer were deposited on the film using e-gun evaporator (ZZS550-2/D, Maestech, Pyeongtaek, Korea). The LCP film was dry etched with oxygen gas using plasma etcher (PlasmaPro System100 Cobra, Oxford Instruments, Abingdon, United Kingdom) for better metal adhesion. Photoresist (AZ4620, MicroChemicals, Ulm, Germany) was spin coated on the film for photolithography. The photoresist was patterned by photolithography using mask aligner (MA-6, SUSS MicroTec, Garching bei München, Germany). On the exposed gold layer, an additional gold layer with thickness of 5 μm was electroplated, and then photoresist and metal seed layers were wet-etched using photoresist remover, a mixture of nitric acid and hydrochloric acid, and hydrofluoric acid solution. Then, the LCP film was detached from the silicon wafer, and laminated with bare LCP films for insulation and thickness-control using heat press (model 4330, Carver, Wabash, USA). The outline of the film was cut with a laser, and the electrode site was ablated with a laser (355 nm UV, Samurai system, DPSS Lasers, Santa Clara, USA).

Fig 2. Fabricated LCP outer box whose shape and size are tailored to the target bone defect.

The structure of the outer box is half cylindrical shell whose cross-section is U-shape. Size of the outer box is 15 mm in length, 7 mm in height, 6 mm in width. Thickness of the shell is 0.35 mm and interconnection line of 5 cm-length is extended for connection to electric stimulator.

This LCP film was then thermoformed using prefabricated molds into a shape that could adapt to the rabbit

150 mandibular bone defect. Two molds were fabricated: the outer mold was designed to possess the shape of the
151 rabbit mandibular body with the created bone defect, and the inner mold was designed to deliver pressure to the
152 LCP film. For the deformation, the LCP film was fixed in the outer mold and heated using the heat press. After
153 the temperature reached 230ºC, the inner mold was inserted in the outer mold to deform the LCP conformably
154 to the surface of the outer mold. The temperature was maintained for 15 minutes before the LCP was cooled
155 down. Then, the LCP was detached from the mold and treated with oxygen plasma followed by cleaning in
156 ethyl alcohol in 60ºC and isopropyl alcohol in 70ºC.

157 After these procedures, the LCP electrodes possessed an identical U shape to the mandibular body surface
158 shape prior to surgical resection, with dimension of 15 mm in length (anterior-posterior), 7 mm in height, and
159 6 mm in depth. The thickness of the LCP was adjusted to be 325 μm to provide sufficient mechanical strength
160 for the maintenance of the defect space. On the inner buccal and lingual surface, gold electrodes were patterned
161 to perform the ES at the bone defect space. The dimension of gold electrodes on both surfaces was 10 x 5 mm^2.
162 To facilitate ingrowth of new vessels and cells for transporting nutrition across the bioreactor, multiple micro-
163 holes (500 μm in diameter) were made, with 2-mm distance between micro-holes. Four macro-holes were made
164 at the upper corners of buccal and lingual LCP sides for the stabilization of the LCP with screws to mandibular
165 bone. An extension plate with 2 mm width and 50 mm length was made for connection with the electrodes from
166 the electric stimulator.

167

168 **Fig 3. Fabricated LCP outer box with gold electrode and macro and micro holes**.

169 Four macro holes are at the edge of the outer box to fix the device with screws at the bone defect. Micro holes
170 are at the surfaces of the outer box to facilitate flow of body fluids between in and out of the box. Two gold
171 electrodes are located at the side walls of the box for electric stimulation.

172

173 **Electric stimulator**

174 Electric stimulator was designed using a custom designed chip (CMOS 0.18 μm foundry, Samsung
175 electronics, Suwon, Korea) previously fabricated [34]. The circuit configuration of the stimulation chip was
176 described in the previous study (24, 25). The integrated chip was wire bonded on the printed circuit board with
177 additional components soldered (25). The biphasic electric current pulses were generated by the electric
178 stimulator, where the parameters of the pulses were set as amplitude of 20 μA, duration of 100 μs, and frequency
179 of 100 Hz. The electric stimulator was connected with the LCP electrode and coin battery (CR1620, Panosonic,
180 Kadoma, Japan) using wire and silver paste. The coin battery and the electric stimulator were packaged using
181 silicone elastomer (MED-6215, Nusil, Carpinteria, USA) for the implantation into the submandibular area.

182

183 **Scaffold**

184 Sterilized absorbable collagen sponge (ACS) sheets (Dalim Tissen Co. Ltd, Seoul, Korea) were cut into
185 rectangle with dimensions of 15 mm width and 7 mm length. Three pieces of absorbable collagen sponge sheets
186 were placed inside the LCP outer box for osteoconductive bone regeneration.

187

188 **Surgical procedure**

189 Fifteen male rabbits (New Zealandia rabbits, 3-3.5 kg weight) were used for the study. Animals were
190 divided into three groups. The control group (n = 5) received neither ES nor rhBMP-2 after the surgery for the
191 implantation of the bioreactor. In the ES group (n = 5), biphasic ES (10 ms time cycle, 100 μs duration, 20 μA
192 amplitude) was applied to the bioreactor for one week immediate after the implantation of bioreactor. In the
193 rhBMP-2 group (n = 5), rhBMP-2 (20 μg /defect) was injected into the defect space one week after the
194 implantation of bioreactor without ES.

195 All animals were treated and handled in accordance with the Recommendations for Handling of Laboratory
196 Animals for Biomedical Research compiled by the Seoul National University Institutional Animal Care and

Use Committee (141120-2). After general anesthesia using Ketamin (20 mg/kg, Yuhan, Seoul, Korea) and Xylazine (Rompun, 10 mg/kg, Bayer, Leverkusen, Germany) and skin disinfection with 10% Povidon-iodinie (Betadine, Purdue Pharma, Stamford, CN, USA), the mandibular body was exposed by incision into the skin and muscle dissection. Defect area to be resected (rectangular shape; 15 mm long, 7 mm high from the mandibular inferior border) was marked on the mandibular bone under the tooth and osteotomized by rotary drilling machine, where alveolar bone with teeth was preserved with continuity with the residual mandibular bone. Because mandibular stabilization with mini-plates after the resection of mandibular body including the alveolar bone with teeth was unstable (25), postoperative dislocation of anterior segment with loosening of mini-plates and screws occurred in our previous experiments due to the strong jaw movement. The bioreactors were positioned into the defect side, stabilized with screws on the neighboring mandibular bone (Fig 4), and the electric stimulator with battery coin were implanted at the submandibular area and then the incision sites were sutured layer by layer. The bioreactor and the electric stimulator remained at the bone defect for the duration of this experiment. Four weeks after the surgery, the animals were sacrificed via an overdose of KCl while animals were in deep anesthesia, and the defect sites, including neighboring bone, were resected for the micro-computer tomography (micro-CT) and histological evaluation. The resected bone tissues were fixed by dipping them in 10 % formalin solution.

Fig 4. Intraoperative photographs and micro CT image after the implantation of bioreactor at the rabbit mandibular bone defect site.

(A) Bone defect was prepared by osteotomy at the mandibular body. (B) The bioreactor was implanted in the defect, where the LCP outer box is fixed on the neighboring bone with two screws. (C) Micro CT image was taken to evaluate newly formed bone.

Micro CT

Micro-CT scan was taken for quantitative evaluation of new bone formation using Skyscan 1172 microfocus X-ray system (Bruker microCT, Kontich, Belgium). The SkyScan 1172 microfocus X-ray system is equipped with a microfocus X-ray tube with a focal spot of 2 mm, producing a cone beam that is detected by a 12-bit cooled X-ray camera CCD fiber optically coupled to a 0.5 mm scintillator. The resulting images were 2,000 x 1,048-pixel square images with an aluminum filter used to produce optimized images. A second-order polynomial correction algorithm was used to reduce the beam-hardening effect for all samples. Reconstructions and analyses were performed using NRecon 1.6.10.4 reconstruction (Bruker microCT, Kontich, Belgium) and CTAn 1.15.4.0 software (Bruker microCT, Kontich, Belgium), respectively. The reconstructed image was rotated three dimensionally for analysis using DataViewer (Bruker microCT, Kontich, Belgium). The 3D image was obtained using CTvol 2.3.1.0 (Bruker microCT, Kontich, Belgium).

In the reconstructed image, bone was isolated from soft tissue and noises by the adjustment of the brightness threshold of the pixel. The threshold between 115 and 230 was used to distinguish bone from noises, soft tissue, and electrode. The predefined defect area was selected as the region of interest (ROI) in two-dimensional images. The pixel zone representing ossification in the defined ROI was then reconstructed in 3D by creating a volume of interest (VOI) in the lower and upper ranges of the threshold using grayscale units. On each reconstructed BMP file, the bone volume per tissue volume (BV/TV), trabecular thickness (Tb.Th), trabecular separation (Tb.Sp), and trabecular number (Tb.N) were obtained using the CTAn 1.15.4.0 software according to the manufacturer's instructions. To measure the bone mineral density (BMD), attenuation data for ROI or VOI were converted to Hounsfield units and expressed as a value of the BMD using a phantom (Bruker microCT, Kontich, Belgium). This phantom contained rods of calcium hydroxyapatite (CaHA) having a standard density corresponding to rabbit bone, which ranges from 1.26 to 1.65 g/cm3. BMD values were expressed in grams per cubic centimeter of CaHA in distilled water. A zero value for BMD corresponded to the density of distilled water alone (no additional CaHA), and a value greater than zero corresponded to non-aerated biologic tissue.

Newly formed bone was evaluated by two different methods. First, it was done in the whole bone defect space. In the second method, it was measured in five subparts; superior-buccal part, inferior-buccal part, superior-lingual part, inferior-lingual part, and central part, as shown in Fig 5. The upper boundaries of superior-

247 buccal and superior-lingual parts were located at the upper surface of the bone defect, and the lower, buccal and
248 lingual boundaries of each subparts were positioned at the lower, buccal and lingual surfaces of the LCP outer
249 box. The central subpart was in the middle part in terms of the buccolingual width and the superior-inferior
250 height of the whole bone defect. The region of interest was 15 mm in length (anterior-posterior), 2 mm in width
251 and 2 mm in height.

252

253 **Fig 5. ROI in the evaluation of new bone formation at the whole bone defect (WD) and at the five subparts.**

254 The size of ROI at subparts is 2 mm in width, 2 mm in height and 15 mm in anterior-posterior length. Subparts
255 are superior-buccal (SB), inferior-buccal (IB), central (C), superior-lingual (SL), and inferior-lingual (IL) parts.

256

257 Histological evaluation

258 After the CT image was taken, the resected bone tissues were further decalcified in an
259 ethylenediaminetetraacetic acid solution (7 %, pH = 7.0) for 1-2 weeks. Then, the tissue samples were immersed
260 in 70% ethanol and embedded in paraffin. For histochemical staining, decalcified paraffin sections were cleaned
261 for 10 min with xylene and stained with Masson's trichrome (MT). The decalcified specimens were sagittally
262 cut at the middle plane of mandibular buccolingual width in the anteroposterior direction of the bone defect.
263 Digital images of the stained sections were collected using a transmission and polarized light Axioscope
264 microscope (Olympus BX51, Olympus Corporation, Tokyo, Japan).

265

266 Statistical analysis

267 The differences among bone parameters in the three groups were first tested using Kruskal Wallis H test
268 and then analyzed using Mann Whitney U test. All statistical analysis was carried out using SPSS software

(SPSS 25, IBM, NY, USA). A p-value < 0.05 was considered to indicate statistically significant differences.

Results and discussion

Macroscopic evaluation

Surgery sites including incision and bone defect area were healed without infection or wound dehiscence. LCP electrodes were maintained in the stabilized position without displacement. No inflammatory signs were seen between skin and bioreactor. All animals could be involved in the evaluation for micro-CT and histology.

Micro-CT analysis

Bone regeneration in whole bone defect

The amount of newly formed bone volume per defect tissue volume (BV/TV) was 132 % greater in the ES group (11.9 ± 1.3 %) ($p < 0.05$) and 174% greater in the rhBMP-2 group (15.8 ± 1.5 %) ($p < 0.01$), compared to the control group (9.0 ± 2.1 %) (Fig 6, Table 1). The new bone was regenerated dominantly near the resected surfaces of the neighboring original mandibular bone. There was less new bone formation at the other areas, with especially poor bone regeneration at the central defect area (Fig 7). Concerning other parameters, Tb.Th and BMD were significantly higher only in the ES group (0.124 ± 0.007 mm and 1.581 ± 0.006 g/cm^3, respectively) compared to those in the control group (0.113 ± 0.008 mm and 1.568 ± 0.010 g/cm^3, respectively) ($p < 0.05$, both). Tb.N was significantly greater only in the rhBMP-2 group (1.34 ± 0.25 mm^{-1}) compared to that in the control group (0.80 ± 0.15 mm^{-1}) ($p < 0.01$). In the comparison between ES and rhBMP-2 groups, BV/TV and Tb.N were significantly higher in the rhBMP-2 group than in the ES group ($p < 0.01$ and $p < 0.05$, respectively). In summary, the rhBMP-2 group was superior in BV/TS and Tb.N compared to the ES group,

while the ES group was superior to the rhBMP-2 group in terms of BMD and Tb.Th (Fig 6).

Fig 6. Analysis of newly formed bone within the whole bone defect in micro-CT evaluation.

The analysis was performed in terms of (A) BV / TV, (B) Tb.Th, (C) Tb.N, (D) Tb.Sp, and (E) BMD. Con; control group without electrical stimulation, ES;cd group with electrical stimulation, rhBMP-2: group with injection of rhBMP-2 without electrical stimulation, BV/TV: bone volume/tissue volume, Tb.Th: trabecular thickness, Tb.N: trabecular number, Tb.Sp: trabecular separation, BMD: bone mineral density. Significant difference between the groups is indicated by *: $p < 0.05$, **: $p<0.01$.

Fig 7. Micro-CT images of the mandibular bone after the experiment.

Micro-CT data was reconstructed in three-dimension to visualize the bone in the rabbit mandibular. The reconstructed image is manipulated by changing blending mode to show (A) mandibular external surface and (B) new bone within bone defect. Bone and gold electrode is depicted brightly, where the defect area is marked with red lines. Con; control group without electrical stimulation, ES; group with electrical stimulation, rhBMP-2: group with injection of rhBMP-2 only without electrical stimulation.

Bone regeneration at five subparts

BV/TV was significantly higher at the superior subparts (34.1 ± 15.8 %) than at the inferior and central subparts (4.7 ± 3.5 % and 2.4 ± 2.2 %, respectively) ($p < 0.01$ for both), and significantly higher at inferior subparts than at central subparts ($p<0.01$). BV/TV at both buccal and lingual subparts (17.8 % and 20.9 %) was significantly greater than that at the central subparts (2.4 ± 2.2 %) ($p < 0.01$ for both), while there was no significant difference in new bone formation between the lingual and buccal subparts (Table 1)

Fig 8. Micro-CT parameters of new bone at the superior-buccal and superior-lingual subparts in the three groups.

The parameters at the superior-buccal subpart include (A) BV/TV, (B) Tb.Th, (C) Tb.N, (D) Tb.Sp, and (E) BMD. Also, the parameters at the superior-lingual subpart include (F) BV/TV, (G) Tb.Th, (H) Tb.N, (I) Tb.Sp, and (J) BMD. Con; control group without electrical stimulation, ES: group with electrical stimulation, rhBMP-2: group with injection of rhBMP-2 only without electrical stimulation. BV: bone volume, TV: tissue volume, Tb.Th: trabecular thickness, Tb.Sp: trabecular separation, Tb.N: trabecular number BMD: bone mineral density. Significant difference between the group is indicated by *: $p < 0.05$, **: $p<0.01$.

The values of BV/TV (%) within five subparts are presented in Table. 1. In the superior subparts, ES and rhBMP-2 groups showed significantly greater BV/TV than in the control group. The superior-buccal subpart showed 205% increased BV/TV in the ES group (32.1 ± 10.5 %) compared to that in the control group (16.2 ± 4.2 %) ($p < 0.05$), while BV/TV in the rhBMP-2 group (48.7 ± 10.8 %) was 301% greater than that in the control group ($p < 0.01$). The superior-lingual subpart showed 239% increased BV/TV in the ES group (39.5%) compared to that in the control group (16.5%) ($p < 0.01$), while BV/TV in the rhBMP-2 group (48.7%) was 310% greater than that in the control group ($p < 0.01$) (Fig 8A, F).

In other parameters of the superior-buccal subpart, Tb.Th and BMD were significantly higher in the ES (0.21 ± 0.08 mm and 1.64 ± 0.04 g/cm^3, respectively) and rhBMP-2 group (0.37 ± 0.13 mm and 1.70 ± 0.05 g/cm^3, respectively) than that in the control group (0.12 ± 0.02 mm and 1.58 ± 0.01 g/cm^3, respectively) ($p < 0.05$ between ES and control group, and $p < 0.01$ between rhBMP-2 and control group) (Fig 8B, E).

In the superior-lingual subpart, Tb.Th was significantly higher in the ES and rhBMP-2 groups (0.19 ± 0.02 mm and 0.24 ± 0.02 mm, respectively) compared to that in the control group (0.12 ± 0.01 mm) ($p < 0.01$ both). Tb.N was significantly higher in the ES and rhBMP-2 groups (2.05 ± 0.22 mm^{-1} and 2.14 ± 0.45 mm^{-1}, respectively) compared to that in the control group (1.39 ± 0.34 mm^{-1}) ($p < 0.05$ both). Tb.Sp was significantly lower in the ES and rhBMP-2 group (0.24 ± 0.05 mm and 0.23 ± 0.07 mm, respectively) compared to that in

338 the control group (0.36 ± 0.10 mm) ($p < 0.05$ both). BMD was significantly higher in the ES and rhBMP-2
339 groups (1.64 ± 0.02 g/cm^3 and 1.66 ± 0.01 g/cm^3, respectively) compared to the control group (1.57 ± 0.01
340 g/cm^3) ($p < 0.01$). (Fig 8G-J).

341 In the inferior and central subparts, there was no significant difference in BV/TV among three groups. The
342 other values of micro-CT parameters and statistical significances are presented in Table 2.

343

344 Table 1. New bone volume per tissue volume (%) within the whole bone defect and five subparts.

Group	Con	ES	rhBMP-2
Whole bone defect	9.0 ± 2.1	11.9 ± 1.3*	15.8 ± 1.5**,★
Superior-buccal part	16.2 ± 4.2	32.1 ± 10.5*	48.7 ± 10.8**,★
Superior-lingual part	16.5 ± 4.8	39.5 ± 6.1**	51.0 ± 10.7**,★
Central part	2.0 ± 1.7	2.3 ± 0.4	2.9 ± 3.7
Inferior-buccal part	2.3 ± 1.5	2.3 ± 0.4	5.1 ± 3.6
Inferior-lingual part	2.9 ± 1.8	6.9 ± 5.1	8.5 ± 6.2*

345

346 Con: control group without electrical stimulation, ES: group with electrical stimulation, rhBMP-2: group with
347 injection of rhBMP-2 only without electrical stimulation.

348 *: $p < 0.05$, **: $p < 0.01$ compared to the control group

349 ★: $p < 0.05$ compared to the ES group

350

351 Table 2. Trabacular bone thickness (mm), Trabacular bone number (1/mm), Trabacular bone separation (mm),
352 and Bone mineral density (g/cm^3) within the central and inferior subparts.

Morphometric parameters	Group	Tb.Th	Tb.N	Tb.Sp	BMD
Superior-buccal part	**Con**	0.12 ± 0.02	1.37 ± 0.42	0.32 ± 0.06	1.58 ± 0.01
	ES	0.21 ± 0.08*	1.62 ± 0.55	0.25 ± 0.04	1.64 ± 0.04*
	rhBMP-2	0.37 ± 0.13**,★	1.41 ± 0.32	0.27 ± 0.10	1.70 ± 0.05**,★
Superior-lingual part	**Con**	0.12 ± 0.01	1.39 ± 0.34	0.36 ± 0.10	1.57 ± 0.01
	ES	0.19 ± 0.02**	2.05 ± 0.22*	0.24 ± 0.05*	1.64 ± 0.02**
	rhBMP-2	0.24 ± 0.02**,★	2.14 ± 0.45*	0.23 ± 0.07*	1.66 ± 0.01**,★
Central part	**Con**	0.072 ± 0.002*	0.27 ± 0.23-	0.60 ± 0.21	1.50 ± 0.01
	ES	0.087 ± 0.023	0.27 ± 0.05	0.47 ± 0.10	1.53 ± 0.03
	rhBMP-2	0.090 ± 0.036	0.25 ± 0.22	0.61 ± 0.15	1.52 ± 0.05
Inferior-buccal part	**Con**	0.076 ± 0.010	0.32 ± 0.21	0.61 ± 0.12	1.50 ± 0.02
	ES	0.075 ± 0.002	0.31 ± 0.05	0.60 ± 0.27	1.51 ± 0.01
	rhBMP-2	0.083 ± 0.009★	0.62 ± 0.44	0.55 ± 0.18	1.52 ± 0.02
Inferior-lingual part	**Con**	0.084 ± 0.008	0.34 ± 0.23	0.71 ± 0.26	1.53 ± 0.003
	ES	0.089 ± 0.019	0.71 ± 0.48*	0.48 ± 0.09	1.53 ± 0.03
	rhBMP-2	0.087 ± 0.011	0.97 ± 0.68*	0.50 ± 0.17	1.53 ± 0.02

Con: control group without electrical stimulation, ES: group with electrical stimulation, rhBMP-2: group with injection of rhBMP-2 only without electrical stimulation.

*: $p < 0.05$, **: $p < 0.01$ compared to the control group

★: $p < 0.05$ compared to the ES group

Histological evaluation

360 The histological images stained in Masson's trichrome showed the new bone regenerated in the bone defect
361 area without inflammation in all groups, and none of the cases showed inflammatory cells at the interface
362 between LCP and newly formed bone area (Fig 9, 10). Interestingly, thin new bone formation was observed
363 along LCP at the inferior bone defect boundary (Fig 9 O, U and Fig 10 A, B, C), and especially thin osteoid
364 layer was seen along LCP surface (Fig 9 B), which indicated a good biocompatibility of LCP for new bone
365 formation. Excessive new bone formation could be seen at the inferior area of LCP in the rhBMP-2 group,
366 probably due to the downward permeation of injected rhBMP-2 through the micro-holes of LCP (Fig 10C). In
367 the control group, most new bone was thin and located near the neighboring bone surface defect with limited
368 new bone ingrowth toward the central part, (Fig 9 A, D-H). In the ES and rhBMP-2 group, new bone was
369 thicker, therefore, more ingrowth into the central part compared to that in the control group was observed (Fig
370 9 B, J-O, C, P-U).

371

372 **Fig 9. Histological images of the regenerated bone (Masson's trichrome staining).**

373 The whole bone defect area is marked by a red rectangular line and the location of the bioreactor is marked in
374 yellow in (A) (Control group), (B) (ES group), and (C) (rhBMP-2 group) (x 12.5). The each location of
375 magnified images (D-H: control group, J-N: ES group, P-T: rhBMP-2, x 100) (I: control group, O: ES group,
376 U: rhBMP-2, x 200) is depicted in A, B, C. The images are taken from different subparts of the defect such as
377 (D, J, P) posterior, (E, I, K, O, Q, U) inferior, (F, L, R) anterior, (G, M, S) superior, and (H) central subpart.
378 New bone has blue color, collagen has red color, extracellular matrix has light blue color, and red blood cells
379 are red dots. Con; control group without electrical stimulation, ES; group with electrical stimulation, rhBMP-2:
380 group with injection of rhBMP-2 only without electrical stimulation.

381

382 **Fig 10**. **Histological images of the regenerated bone area contacted with the surface of the LCP outerbox**
383 **in inferior-central region.**

384 Location of LCP outer box is marked in yellow. There were no inflammatory reactions in newly regenerated
385 bone in (A) CON, (B) EC, (C) rhBMP-2 group (Masson's trichrome staining, magnification x500). New bone
386 as blue color, collagen as red color, extracellular matrix as light blue color, red blood cells as red dots.

387

388 # Discussion

389 This study addressed the effect of an *in vivo* bone bioreactor with ES on the bone regeneration at a large
390 mandibular defect. We designed the bioreactor which was connected to custom-made electrodes based on LCP
391 without stem cells or growth factor. LCP had multifunctional capacities and was biocompatible with bone, as
392 well as mechanically stable to hold the shape of the bioreactor. Our bioreactor system is based on the previous
393 reports that biphasic ES increased cell proliferation of human stem cells (hMSC) and several growth factors
394 such as vascular endothelial growth factor (VEGF), BMP-2, and -interleukin-8 (24, 25). These properties
395 provide a great potential to create favorable microenvironments for bone regeneration. VEGF is a critical factor
396 for angiogenesis, and IL-8 is a chemokine to recruit stem cells. This *in vivo* bioreactor system with ES benefits
397 from one-staged direct application compared to a two-staged procedure where first the bioreactor is transplanted
398 to the well-vascularized heterotopic sites prefabricated, and then, the regenerated tissue is transplanted to the
399 orthotopic site (32, 33).

400 The timing and duration of ES and BMP-2 treatment is an important aspect of experimental design for the
401 optimal results. The effect of the ES in bone cells is different in different stages of cell maturation (34). Further,
402 the effect of the rhBMP-2 varies in different stages of bone cells (35). The ES was conducted for one week
403 after surgery, and BMP-2 was applied one week after surgery in this present study, based on reports that bone
404 cell culture showed active proliferation but rare mineral deposition in the first week, while deposition was
405 observed with declined proliferation after two weeks (36, 37). In addition, after fracture, cell proliferation lasted
406 for 7 days, and then the cell differentiation and bone fusion occurred (38). Furthermore, in the animal experiment
407 with ES and BMP-2 (25), new bone formation was significantly higher in the group where BMP-2 application
408 as delayed until one week after ES compared to that in the group with simultaneous application of ES and BMP-

409 2. It seems that delayed BMP-2 application after the cell proliferation period is more efficient than immediate
410 application after surgery.

411 Liquid crystal polymer (LCP) is a biocompatible material (39, 40) and its mechanical strength is similar to
412 that of the bone (31, 41, 42). The tensile strength of LCP and cortical bone is 240 MPa and 150 MPa, respectively.
413 The Young's modulus of LCP and cortical bone is 2 GPa and 7 GPa, respectively. Because of the similarity in
414 the mechanical strength and a good fixation-to-bone property (43), this material is considered adequate for
415 orthopedic applications (44). Furthermore it is chemically inert, allows hermetic sealing, and is compatible with
416 MEMS microfabrication process with multilayer integration (45-48). LCP-based packaging of a neural
417 prosthetic device was studied (49-51). Because of its thermo-forming property, it also allows the shape of the
418 device to be formed to fit the target volume. This is the first report of an LCP-based electrode being used for
419 bone regeneration. LCP based electrode was used for both ES and mechanical support of scaffolds. The
420 electrode had good mechanical characteristic for bone regeneration, and the volume of newly formed bone was
421 higher than with our previous ES device based on polyimide (25). Further, histochemical staining showed no
422 inflammation, suggesting that LCP is biocompatible. Micro CT images showed the bones formed on the outer
423 and inner surfaces of the LCP. Histochemical staining demonstrated the new bone formation near the surfaces
424 of the LCP. Our study suggested that electric stimulation with the implanted bioreactor based on LCP was
425 effective in bone regeneration.

426 ES has been widely used as a method to enhance bone regeneration (52-54) and nerve regeneration (49, 55).
427 ES increases proliferation, calcium deposition, and alkaline phosphate activity of bone related cells (56, 57)ES
428 is known to open voltage gated calcium channels to increase intra-cellular calcium ions (58), which activates
429 the cytoskeletal calmodulin (27). Increased calcium level might lead to an increased nitric oxide levels, which
430 acts in a physiological context through increased synthesis of cGMP and subsequent activation of protein kinase
431 G, which was associated with cell division and nucleic acid synthesis (59). ES also made the cellular
432 environment more suitable for osteogenesis (25). The effect of ES included increased gene expression of type I
433 collagen and prostaglandin (57), growth factors (BMP-2, IGF-1, VEGF), and chemokines with receptors (24).
434 ES activates mitogen-activated protein kinase (MAPK) and calcium channels, leading to increased induction of

435 VEGF and BMP-2 of bone cells (28, 57). Additionally, ES increases TGF-β1 through the calcium calmodulin
436 pathway (60). In the present study, micro-CT evaluation showed that the bone volume in the ES group was 132
437 % that of the control group. This result matched that of our previous experiment of ES in a dental implant, where
438 the bone area in the ES group was 130 to 135 % of bone area in control group (28). Even though ES could
439 stimulate new bone regeneration, its effect on the amount of new bone formation was less than rhBMP-2 applied
440 one week after surgery. It seems that enhanced cell differentiation by BMP-2 of small cell numbers is more
441 efficient in bone regeneration than enhanced cell proliferation and differentitation by ES. However, Tb.Th and
442 BMD were significantly higher only in the ES group compared to the control group, while there was no
443 significant difference between the rhBMP-2 and control groups. These results suggests that new bone formation
444 would be further enhanced in cases with initial ES for one week followed by rhBMP-2 application.

445 The effect of stimuli like ES or rhBMP-2 on bone regeneration can be different depending on the abundance
446 of vascularity and stem cells. Corresponding to this expectation, new bone formation was predominant at the
447 defect space adjacent to the existing host mandibular bone in the present study. Bone regeneration by ES was
448 highest at the superior subpart of the bone defect than other subparts. This subpart was covered with more
449 adjacent host bone surface including upper defect surface, providing more chance for stimulation of preexisting
450 blood vessels and stem cells by proximal electrode. Based on the fact that electric current density is at is
451 maximum near the electrode and gradually decreased as moving far from the electrode (61), and that the amount
452 of the charge delivered is proportional to the amount of newly formed bone (62), more new bone could be
453 observed near LCP. Considering that electric current can only flow through the conductive medium, it seems
454 that host bone and newly regenerated tissue adjacent to bone defect are non-conductive substances. Blood clots
455 and body fluid, which filled the bone defect space after surgery, may be electrically a conductive medium, but
456 bone regeneration at the bone defect space far from existing host bone was poor , even with ES or rhBMP-2,
457 because they could only be effective at the bone defect with infiltrated stem cells and ingrowing blood vessels.
458 Vascularization is important for osteogenesis in large bone defect (63, 64). Biphasic electric pulse is effective
459 for the increased secretion of VEGF from osteoblasts and stem cells (65), which is essential in angiogenesis
460 (66) andstimulates new bone formation by osteoblasts (67). Slow and steady release of VEGF promotes in bone

formation (68), which can be effectively achieved through electric stimulation. On the other hand, the effect of ES or rhBMP-2 on bone regeneration can be influenced by the delivery efficacy of stimuli. According to the results of the present study and previous animal experimentation (25), initial ES followed by delayed BMP-2 application would be more efficient than ES or delayed BMP-2 application alone.

Conclusions

We verified the intracorporeally implanted ES bioreactor with LCP electrodes for bone regeneration, where LCP can act as a mechanically resistant outer box in bone defect without inflammation. The bioreactor system with ES significantly increased new bone formation compared to the control without ES at a large bone defect of rabbit mandible. The bioreactor system with ES was superior in BMD compared to rhBMP-2, while rhBMP-2 applied one week after surgery showed more enhanced osteogenesis than the bioreactor system with ES. Further experiments with other conditions of the bioreactor may be helpful to develop more effective bone regeneration.

Financial disclosures

This work was supported in part by the Dentistry - Engineering Interdisciplinary Research Grant jointly funded by the School of Dentistry and College of Engineering, Seoul National University; and in part by a grant to CABMC project funded by the Defense Acquisition Program Administration (UD170030ID)

References

1. Giannoudis PV, Einhorn TA, Marsh D. Fracture healing: the diamond concept. Injury. 2007;38:S3-S6.
2. Chao E, Inoue N. Biophysical stimulation of bone fracture repair, regeneration and remodelling. Eur

483 Cell Mater. 2003;6:72-84.
484 3. Kashte S, Jaiswal AK, Kadam S. Artificial bone via bone tissue engineering: current scenario and
485 challenges. Tissue Engineering and Regenerative Medicine. 2017;14(1):1-14.
486 4. Sobhani A, Rafienia M, Ahmadian M, Naimi-Jamal M-R. Fabrication and Characterization of
487 Polyphosphazene/Calcium Phosphate Scaffolds Containing Chitosan Microspheres for Sustained Release of
488 Bone Morphogenetic Protein 2 in Bone Tissue Engineering. Tissue Engineering and Regenerative Medicine.
489 2017;14(5):525-38.
490 5. Kim IS, Cho TH, Lee ZH, Hwang SJ. Bone regeneration by transplantation of human mesenchymal
491 stromal cells in a rabbit mandibular distraction osteogenesis model. Tissue engineering Part A. 2013;19(1-
492 2):66-78.
493 6. Yoon Y, Khan IU, Choi KU, Jung T, Jo K, Lee S-H, et al. Different Bone Healing Effects of
494 Undifferentiated and Osteogenic Differentiated Mesenchymal Stromal Cell Sheets in Canine Radial Fracture
495 Model. Tissue Engineering and Regenerative Medicine. 2018;15(1):115-24.
496 7. Bueno EM, Glowacki J. Cell-free and cell-based approaches for bone regeneration. Nature Reviews
497 Rheumatology. 2009;5(12):685.
498 8. Ankrum J, Karp JM. Mesenchymal stem cell therapy: Two steps forward, one step back. Trends in
499 Molecular Medicine. 2010;16(5):203-9.
500 9. Jafarian M, Eslaminejad MB, Khojasteh A, Mashhadi Abbas F, Dehghan MM, Hassanizadeh R, et al.
501 Marrow-derived mesenchymal stem cells-directed bone regeneration in the dog mandible: a comparison
502 between biphasic calcium phosphate and natural bone mineral. Oral Surgery, Oral Medicine, Oral Pathology,
503 Oral Radiology, and Endodontology. 2008;105(5):e14-e24.
504 10. Lim J, Razi ZRM, Law JX, Nawi AM, Idrus RBH, Chin TG, et al. Mesenchymal Stromal Cells from the
505 Maternal Segment of Human Umbilical Cord is Ideal for Bone Regeneration in Allogenic Setting. Tissue
506 Engineering and Regenerative Medicine. 2018;15(1):75-87.
507 11. Urist MR, Strates BS. Bone morphogenetic protein. Journal of dental research. 1971;50(6):1392-406.
508 12. Ha W-H, Seong H-S, Choi N-R, Park B-S, Kim Y-D. Recombinant human bone morphogenic protein-
509 2 Induces the Differentiation and Mineralization of Osteoblastic Cells Under Hypoxic Conditions via
510 Activation of Protein Kinase D and p38 Mitogen-Activated Protein Kinase Signaling Pathways. Tissue
511 Engineering and Regenerative Medicine. 2017;14(4):433-41.
512 13. Kim SK, Cho TH, Han JJ, Kim IS, Park Y, Hwang SJ. Comparative study of BMP-2 alone and combined
513 with VEGF carried by hydrogel for maxillary alveolar bone regeneration. Tissue Engineering and Regenerative
514 Medicine. 2016;13(2):171-81.
515 14. Kim K, Kim IS, Cho TH, Seo YK, Hwang SJ. High-intensity Nd: YAG laser accelerates bone
516 regeneration in calvarial defect models. Journal of tissue engineering and regenerative medicine.
517 2015;9(8):943-51.
518 15. Hwang SJ, Lublinsky S, Seo Y-K, Kim IS, Judex S. Extremely small-magnitude accelerations enhance
519 bone regeneration: a preliminary study. Clinical orthopaedics and related research. 2009;467(4):1083-91.
520 16. Kim IS, Lee EN, Cho TH, Song YM, Hwang SJ, Oh JH, et al. Promising efficacy of Escherichia coli

521 recombinant human bone morphogenetic protein-2 in collagen sponge for ectopic and orthotopic bone
522 formation and comparison with mammalian cell recombinant human bone morphogenetic protein-2. Tissue
523 Engineering Part A. 2010;17(3-4):337-48.
524 17. Song W-Y, Liu G-M, Li J, Luo Y-G. Bone morphogenetic protein-2 sustained delivery by hydrogels
525 with microspheres repairs rabbit mandibular defects. Tissue Engineering and Regenerative Medicine.
526 2016;13(6):750-61.
527 18. Shields LBE, Raque GH, Glassman SD, Campbell M, Vitaz T, Harpring J, et al. Adverse Effects
528 Associated With High-Dose Recombinant Human Bone Morphogenetic Protein-2 Use in Anterior Cervical
529 Spine Fusion. Spine. 2006;31(5):542-7.
530 19. Mesfin A, Buchowski JM, Zebala LP, Bakhsh WR, Aronson AB, Fogelson JL, et al. High-dose rhBMP-2
531 for adults: major and minor complications: a study of 502 spine cases. JBJS. 2013;95(17):1546-53.
532 20. Zara JN, Siu RK, Zhang X, Shen J, Ngo R, Lee M, et al. High Doses of Bone Morphogenetic Protein
533 2 Induce Structurally Abnormal Bone and Inflammation In Vivo. Tissue Engineering Part A. 2011;17(9-
534 10):1389-99.
535 21. Kim RY, Oh JH, Lee BS, Seo Y-K, Hwang SJ, Kim IS. The effect of dose on rhBMP-2 signaling,
536 delivered via collagen sponge, on osteoclast activation and in vivo bone resorption. Biomaterials.
537 2014;35(6):1869-81.
538 22. Cho TH, Kim IS, Lee B, Park SN, Ko JH, Hwang SJ. (*) Early and Marked Enhancement of New Bone
539 Quality by Alendronate-Loaded Collagen Sponge Combined with Bone Morphogenetic Protein-2 at High
540 Dose: A Long-Term Study in Calvarial Defects in a Rat Model. Tissue engineering Part A. 2017;23(23-
541 24):1343-60.
542 23. Huang R-L, Kobayashi E, Liu K, Li Q. Bone graft prefabrication following the in vivo bioreactor
543 principle. EBioMedicine. 2016;12:43-54.
544 24. Kim J, Lee TH, Song YM, Kim IS, Cho TH, Hwang SJ, et al. An implantable electrical bioreactor for
545 enhancement of cell viability. Proceedings of 2011 Annual International Conference of the IEEE Engineering
546 in Medicine and Biology Society; 2011 Aug 30 – Sep 3; Boston, MA, USA. IEEE; 2011.
547 25. Kim J, Yang HJ, Cho TH, Lee SE, Park YD, Kim HM, et al. Enhanced regeneration of rabbit mandibular
548 defects through a combined treatment of electrical stimulation and rhBMP-2 application. Medical &
549 biological engineering & computing. 2013;51(12):1339-48.
550 26. Cai S, Bodle JC, Mathieu PS, Amos A, Hamouda M, Bernacki S, et al. Primary cilia are sensors of
551 electrical field stimulation to induce osteogenesis of human adipose-derived stem cells. The FASEB Journal.
552 2017;31(1):346-55.
553 27. Balint R, Cassidy NJ, Cartmell SH. Electrical stimulation: a novel tool for tissue engineering. Tissue
554 Engineering Part B: Reviews. 2012;19(1):48-57.
555 28. Kim IS, Song JK, Song YM, Cho TH, Lee TH, Lim SS, et al. Novel effect of biphasic electric current
556 on in vitro osteogenesis and cytokine production in human mesenchymal stromal cells. Tissue Engineering
557 Part A. 2009;15(9):2411-22.
558 29. Jeong J, Bae SH, Seo J-M, Chung H, Kim SJ. Long-term evaluation of a liquid crystal polymer (LCP)-

559 based retinal prosthesis. Journal of neural engineering. 2016;13(2):025004.
560 30. Shin S, Kim J-H, Jeong J, Gwon TM, Lee S-H, Kim SJ. Novel four-sided neural probe fabricated by
561 a thermal lamination process of polymer films. Journal of neuroscience methods. 2017;278:25-35.
562 31. Kettunen J, Mäkelä A, Miettinen H, Nevalainen T, Pohjonen T, Suokas E, et al. The fixation properties
563 of carbon fiber-reinforced liquid crystalline polymer implant in bone: An experimental study in rabbits.
564 Journal of biomedical materials research. 2001;56(1):137-43.
565 32. Wiltfang J, Rohnen M, Egberts J-H, Lützen U, Wieker H, Açil Y, et al. Man as a living bioreactor:
566 prefabrication of a custom vascularized bone graft in the gastrocolic omentum. Tissue Engineering Part C:
567 Methods. 2016;22(8):740-6.
568 33. Han D, Dai K. Prefabrication of a vascularized bone graft with Beta tricalcium phosphate using an
569 in vivo bioreactor. Artificial organs. 2013;37(10):884-93.
570 34. Diniz P, Shomura K, Soejima K, Ito G. Effects of pulsed electromagnetic field (PEMF) stimulation on
571 bone tissue like formation are dependent on the maturation stages of the osteoblasts. Bioelectromagnetics.
572 2002;23(5):398-405.
573 35. Kim IS, Song YM, Cho TH, Park YD, Lee KB, Noh I, et al. In vitro response of primary human bone
574 marrow stromal cells to recombinant human bone morphogenic protein-2 in the early and late stages of
575 osteoblast differentiation. Development, growth & differentiation. 2008;50(7):553-64.
576 36. Kim S, Das S, Lee H, Kim J, Song YM, Kim IS, et al. Preliminary approach of real-time monitoring in
577 vitro matrix mineralization based on surface plasmon resonance detection. Biotechnology and
578 bioengineering. 2011;108(6):1473-8.
579 37. Dworetzky SI, Fey EG, Penman S, Lian JB, Stein JL, Stein GS. Progressive changes in the protein
580 composition of the nuclear matrix during rat osteoblast differentiation. Proceedings of the National
581 Academy of Sciences. 1990;87(12):4605-9.
582 38. Tatsuyama K, Maezawa Y, Baba H, Imamura Y, Fukuda M. Expression of various growth factors for
583 cell proliferation and cytodifferentiation during fracture repair of bone. European journal of histochemistry:
584 EJH. 2000;44(3):269.
585 39. Bae SH, Che J-H, Seo J-M, Jeong J, Kim ET, Lee SW, et al. In vitro biocompatibility of various
586 polymer-based microelectrode arrays for retinal prosthesismicroelectrode arrays for retinal prosthesis.
587 Investigative ophthalmology & visual science. 2012;53(6):2653-7.
588 40. Shin S, Kim J-H, Jeong J, Gwon TM, Lee S-H, Kim SJ. Novel four-sided neural probe fabricated by
589 a thermal lamination process of polymer films. Journal of Neuroscience Methods. 2016;278:25-35.
590 41. Shin S, Kim J, Jeong J, Gwon TM, Choi GJ, Lee SE, et al. High Charge Storage Capacity
591 Electrodeposited Iridium Oxide Film on Liquid Crystal Polymer-Based Neural Electrodes. Sensors and
592 Materials. 2016;28(3):243-60.
593 42. Jeong J, Lee SW, Min K, Eom K, Bae SH, Kim SJ. Eye-surface conformable telemetric structure for
594 polymer-based retinal prosthesis. Proceedings of 2011 Annual International Conference of the IEEE
595 Engineering in Medicine and Biology Society; 2011 Aug 30 – Sep 3; Boston, MA, USA. IEEE; 2011.
596 43. Kettunen J, Mäkeläa E, Miettinen H, Nevalainen T, Heikkilä M, Pohjonen T, et al. Mechanical

properties and strength retention of carbon fibre-reinforced liquid crystalline polymer (LCP/CF) composite: an experimental study on rabbits. Biomaterials. 1998;19(14):1219-28.

44. Kim J. Development of an Implantable Electrical Stimulation Device for Bone Regeneration. Dr.Sc. Dissertation, Seoul National University, 2014. Available from: http://dcollection.snu.ac.kr/jsp/common/DcLoOrgPer.jsp?sItemId=000000021298

45. Seo J, Wee JH, Park JH, Park P, Kim J-W, Kim SJ. Nerve cuff electrode using embedded magnets and its application to hypoglossal nerve stimulation. Journal of Neural Engineering. 2016;13(6):066014.

46. Gwon TM, Min KS, Kim JH, Oh SH, Lee HS, Park M-H, et al. Fabrication and evaluation of an improved polymer-based cochlear electrode array for atraumatic insertion. Biomedical microdevices. 2015;17(2):1-12.

47. Jeong J, Bae SH, Min KS, Seo J-M, Chung H, Kim SJ. A miniaturized, eye-conformable, and long-term reliable retinal prosthesis using monolithic fabrication of liquid crystal polymer (LCP). IEEE Transactions on Biomedical Engineering. 2015;62(3):982-9.

48. Lee SW, Seo J-M, Ha S, Kim ET, Chung H, Kim SJ. Development of microelectrode arrays for artificial retinal implants using liquid crystal polymers. Investigative ophthalmology & visual science. 2009;50(12):5859-66.

49. Kim IS, Song YM, Cho TH, Pan H, Lee TH, Kim SJ, et al. Biphasic electrical targeting plays a significant role in schwann cell activation. Tissue Engineering Part A. 2011;17(9-10):1327-40.

50. Park JH, Jeong J, Moon H, Kim C, Kim SJ. Feasibility of LCP as an Encapsulating Material for Photodiode-Based Retinal Implants. IEEE Photonics Technology Letters. 2016;28(9):1018-21.

51. Min KS, Oh SH, Park M-H, Jeong J, Kim SJ. A polymer-based multichannel cochlear electrode array. Otology & Neurotology. 2014;35(7):1179-86.

52. Lavine L, Lustrin I, Shamos M, Moss M. The influence of electric current on bone regeneration in vivo. Acta Orthopaedica Scandinavica. 1971;42(4):305-14.

53. Levy DD, Rubin B. Inducing bone growth in vivo by pulse stimulation. Clinical orthopaedics and related research. 1972;88:218-22.

54. Buch F, Albrektsson T, Herbst E. Direct current influence on bone formation in titanium implants. Biomaterials. 1984;5(6):341-6.

55. Lee TH, Pan H, Kim IS, Kim JK, Cho TH, Oh JH, et al. Functional Regeneration of a Severed Peripheral Nerve With a 7-mm Gap in Rats Through the Use of An Implantable Electrical Stimulator and a Conduit Electrode With Collagen Coating. Neuromodulation: Technology at the Neural Interface. 2010;13(4):299-305.

56. Ercan B, Webster TJ. The effect of biphasic electrical stimulation on osteoblast function at anodized nanotubular titanium surfaces. Biomaterials. 2010;31(13):3684-93.

57. Kim IS, Song JK, Zhang YL, Lee TH, Cho TH, Song YM, et al. Biphasic electric current stimulates proliferation and induces VEGF production in osteoblasts. Biochimica et Biophysica Acta (BBA)-Molecular Cell Research. 2006;1763(9):907-16.

58. Brighton CT, Wang W, Seldes R, Zhang G, Pollack SR. Signal transduction in electrically stimulated bone cells. J Bone Joint Surg Am. 2001;83(10):1514-23.

59. Pall ML. Electromagnetic fields act via activation of voltage-gated calcium channels to produce beneficial or adverse effects. Journal of cellular and molecular medicine. 2013;17(8):958-65.

60. Zhuang H, Wang W, Seldes RM, Tahernia AD, Fan H, Brighton CT. Electrical stimulation induces the level of TGF-β1 mRNA in osteoblastic cells by a mechanism involving calcium/calmodulin pathway. Biochemical and biophysical research communications. 1997;237(2):225-9.

61. Purcell EM, Morin DJ. Electricity and magnetism. 3rd ed. Cambridge University Press; 2013.

62. Brighton CT, Friedenberg ZB, Black J, ESTERHAI Jr JL, Mitchell JEI, MONTIQUE Jr F. Electrically induced osteogenesis: relationship between charge, current density, and the amount of bone formed: introduction of a new cathode concept. Clinical orthopaedics and related research. 1981;161:122-32.

63. Mercado-Pagán ÁE, Stahl AM, Shanjani Y, Yang Y. Vascularization in bone tissue engineering constructs. Annals of biomedical engineering. 2015;43(3):718-29.

64. Glowacki J. Angiogenesis in fracture repair. Clinical orthopaedics and related research. 1998;355:S82-S9.

65. Kim IS, Song JK, Zhang YL, Lee TH, Cho TH, Song YM, et al. Biphasic electric current stimulates proliferation and induces VEGF production in osteoblasts. Biochimica et Biophysica Acta (BBA) - Molecular Cell Research. 2006;1763(9):907-16.

66. Maes C, Carmeliet P, Moermans K, Stockmans I, Smets N, Collen D, et al. Impaired angiogenesis and endochondral bone formation in mice lacking the vascular endothelial growth factor isoforms VEGF 164 and VEGF 188. Mechanisms of development. 2002;111(1):61-73.

67. Zelzer E, McLean W, Ng Y-S, Fukai N, Reginato AM, Lovejoy S, et al. Skeletal defects in VEGF120/120 mice reveal multiple roles for VEGF in skeletogenesis. Development. 2002;129(8):1893-904.

68. Street J, Bao M, Bunting S, Peale FV, Ferrara N, Steinmetz H, et al. Vascular endothelial growth factor stimulates bone repair by promoting angiogenesis and bone turnover. Proceedings of the National Academy of Sciences. 2002;99(15):9656-61.

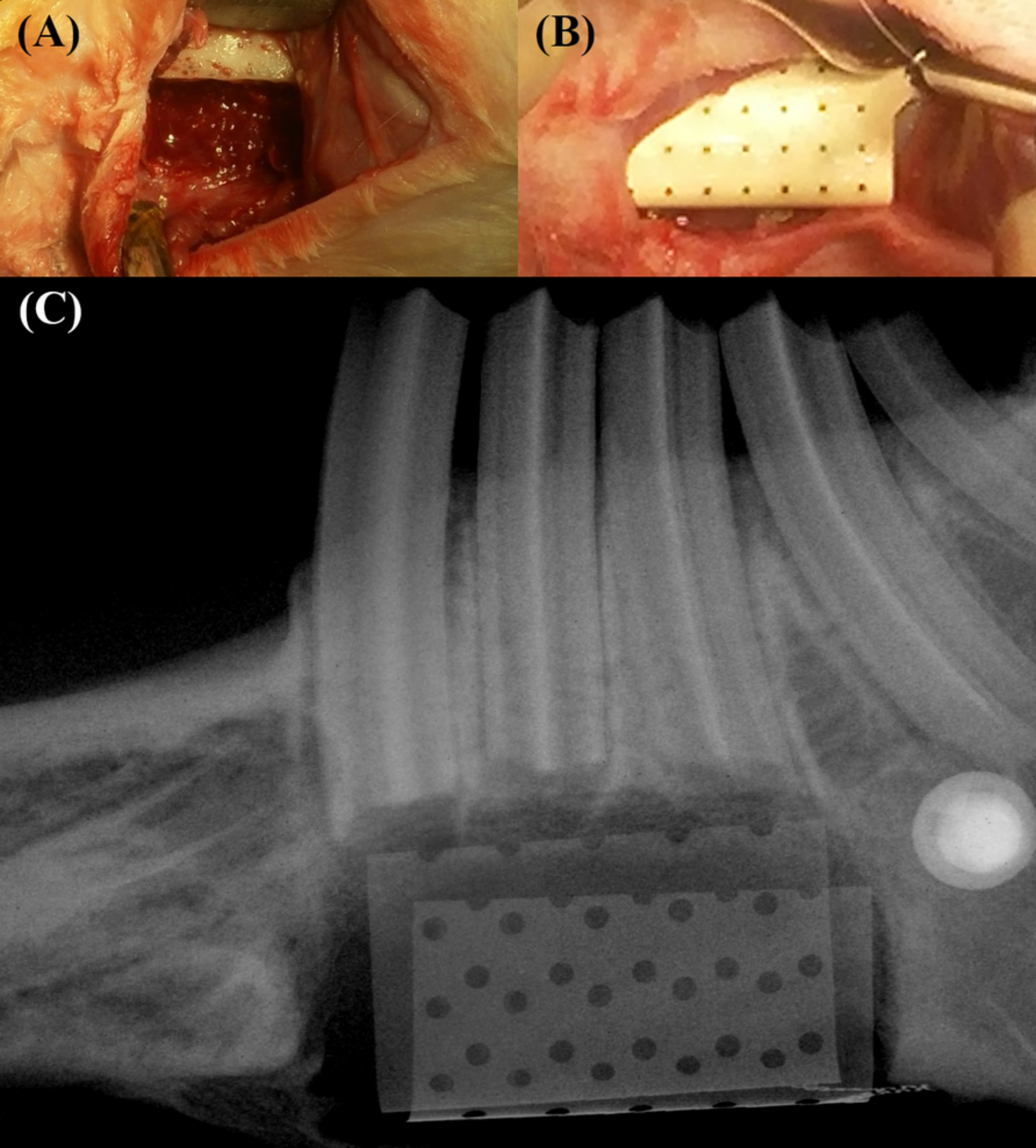
(A)
(B)
(C)

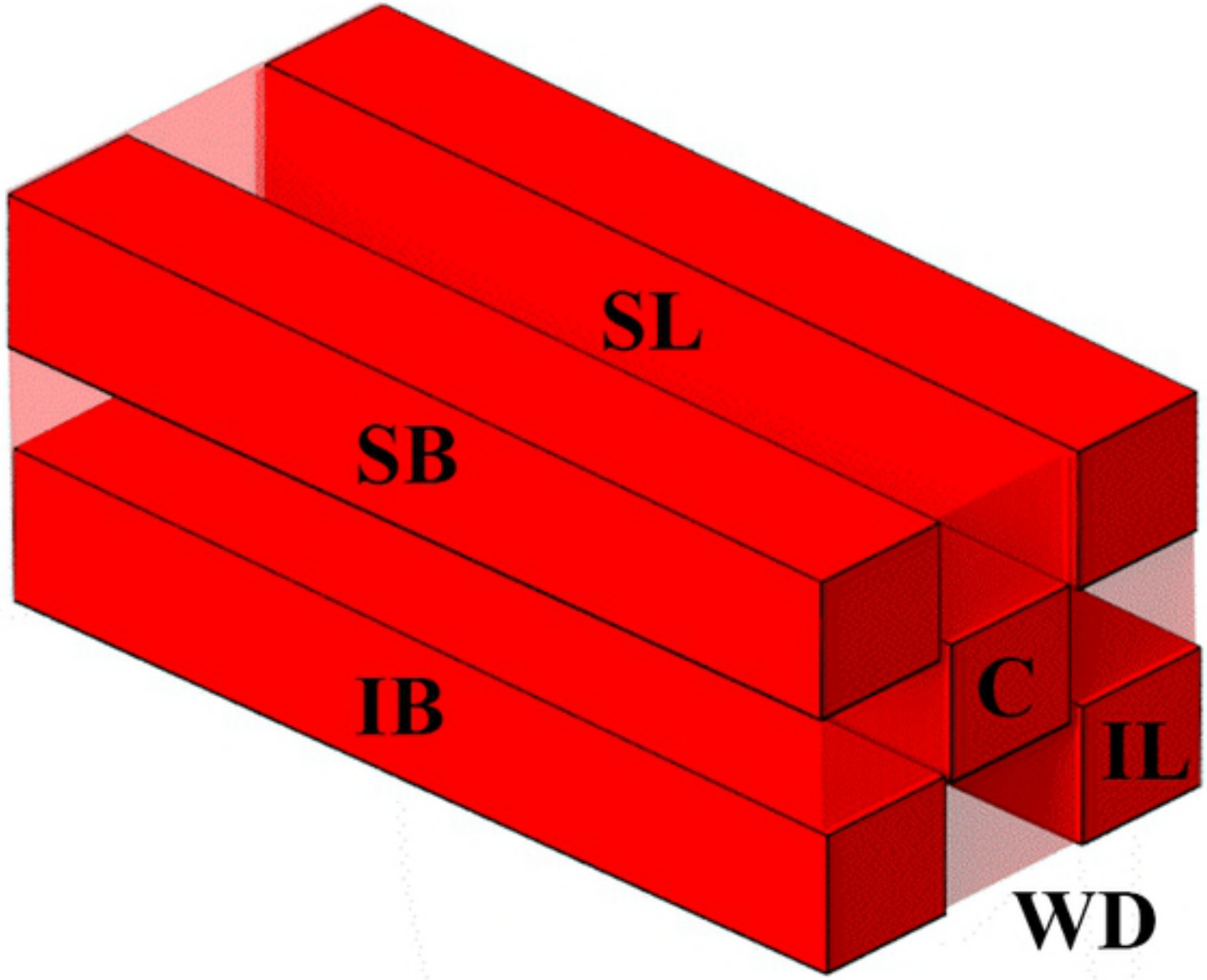
SL
SB
IB
C
IL
WD

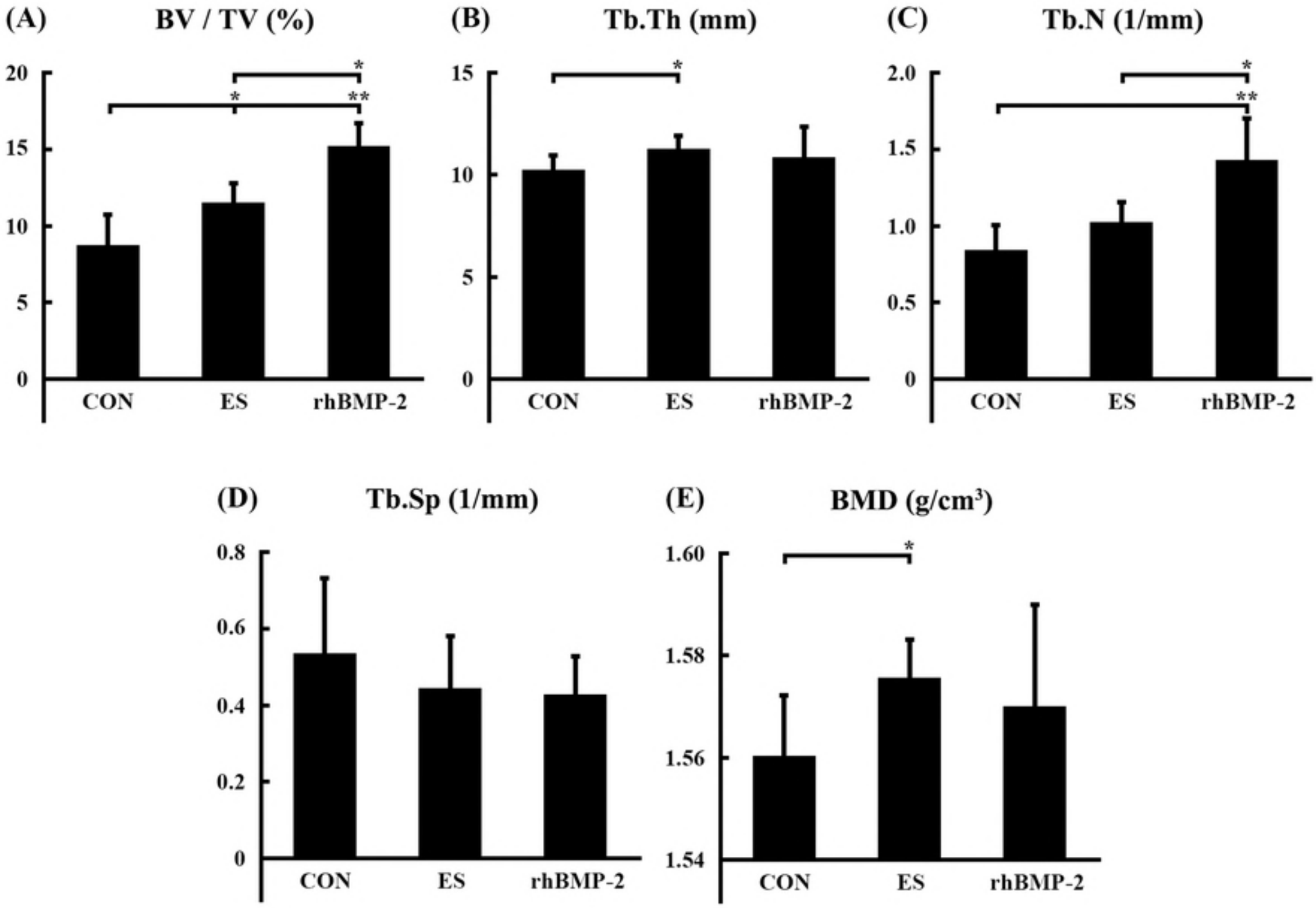
(A)
BV / TV (%)
20
15
10
5
0
*
*
**
CON
ES
rhBMP-2
(B)
Tb.Th (mm)
15
10
5
0
*
CON
ES
rhBMP-2
(C)
Tb.N (1/mm)
2.0
1.5
1.0
0.5
0
*
**
CON
ES
rhBMP-2
(D)
Tb.Sp (1/mm)
0.8
0.6
0.4
0.2
0
CON
ES
rhBMP-2
(E)
BMD (g/cm3)
1.60
1.58
1.56
1.54
*
CON
ES
rhBMP-2

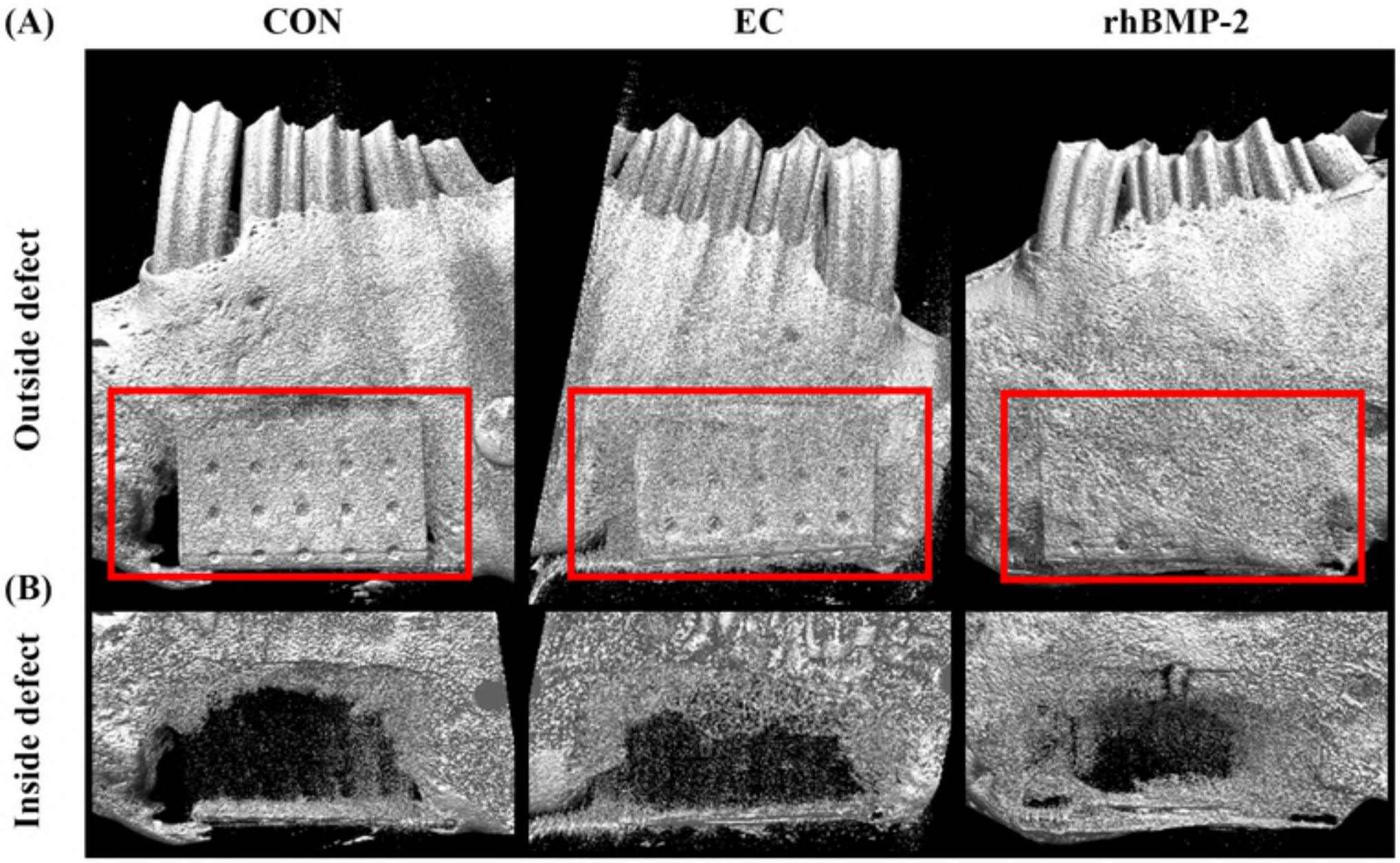
(A)
CON
EC
rhBMP-2
Outside defect
(B)
Inside defect

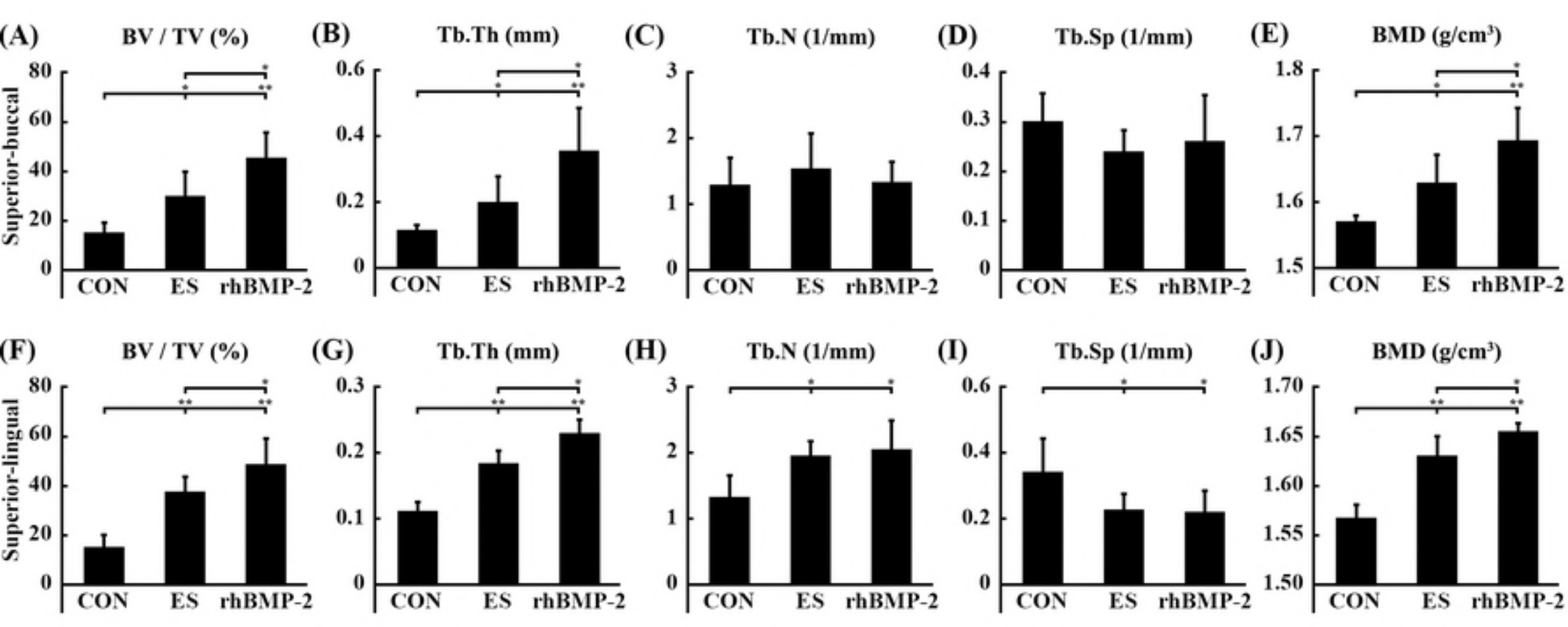
(A)
BV / TV (%)
Superior-buccal
(B)
Tb.Th (mm)
(C)
Tb.N (1/mm)
(D)
Tb.Sp (1/mm)
(E)
BMD (g/cm³)
(F)
BV / TV (%)
Superior-lingual
(G)
Tb.Th (mm)
(H)
Tb.N (1/mm)
(I)
Tb.Sp (1/mm)
(J)
BMD (g/cm³)
CON
ES
rhBMP-2

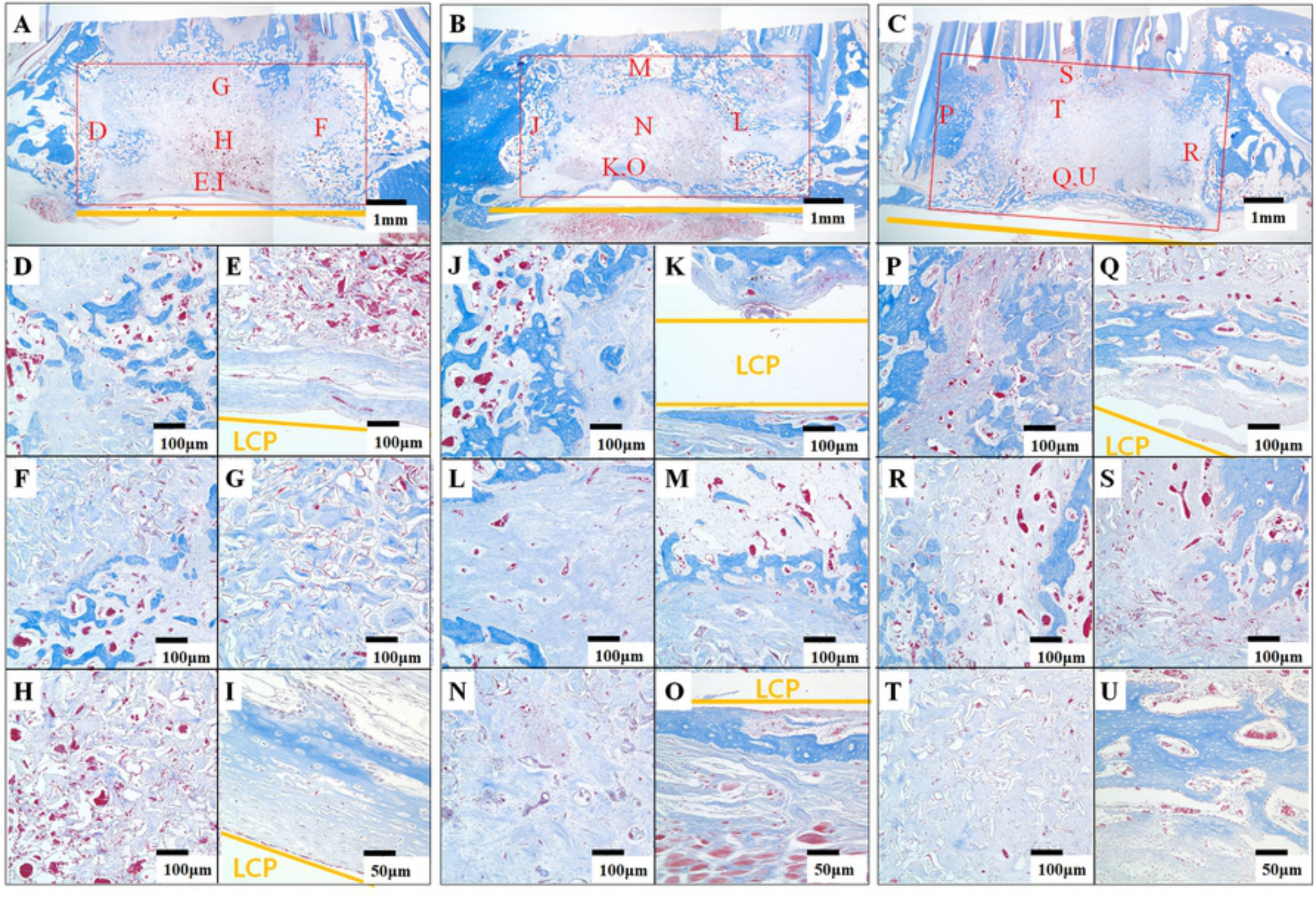
A
G
D
H
F
E,I
1mm
B
M
J
N
L
K,O
1mm
C
S
P
T
R
Q,U
1mm
D
100μm
E
LCP
100μm
J
100μm
K
LCP
100μm
P
100μm
Q
LCP
100μm
F
100μm
G
100μm
L
100μm
M
100μm
R
100μm
S
100μm
H
100μm
I
LCP
50μm
N
100μm
O
LCP
50μm
T
100μm
U
50μm

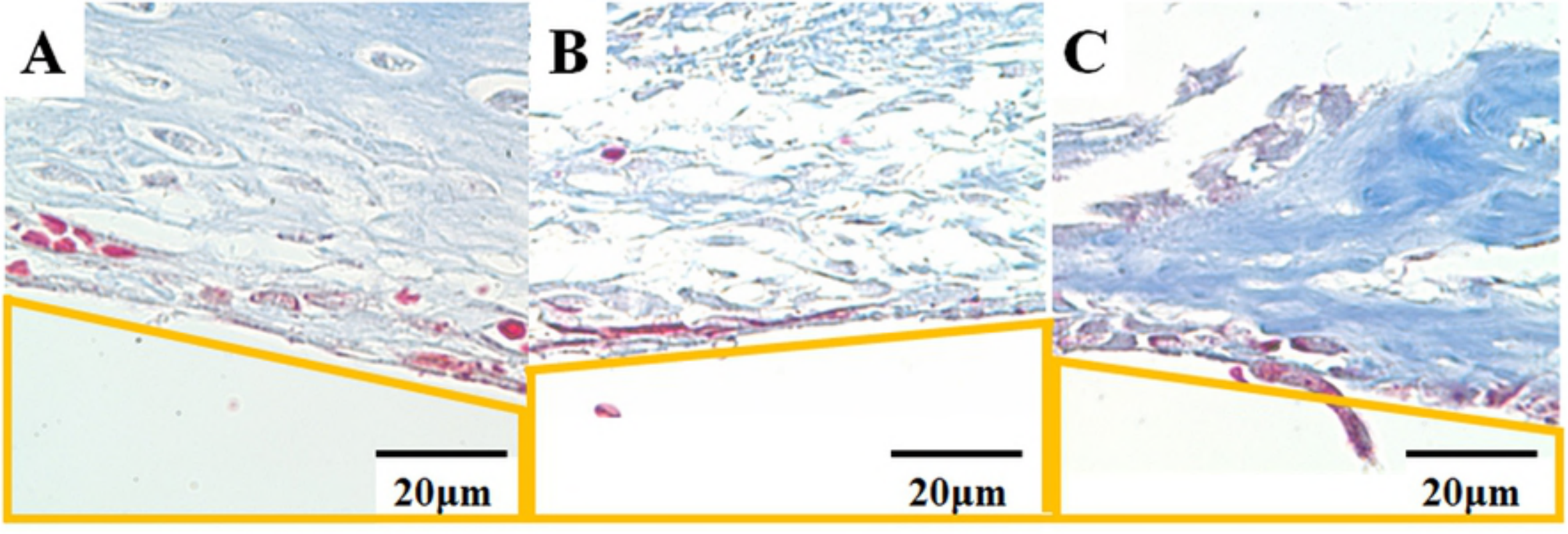
A
B
C
20μm
20μm
20μm

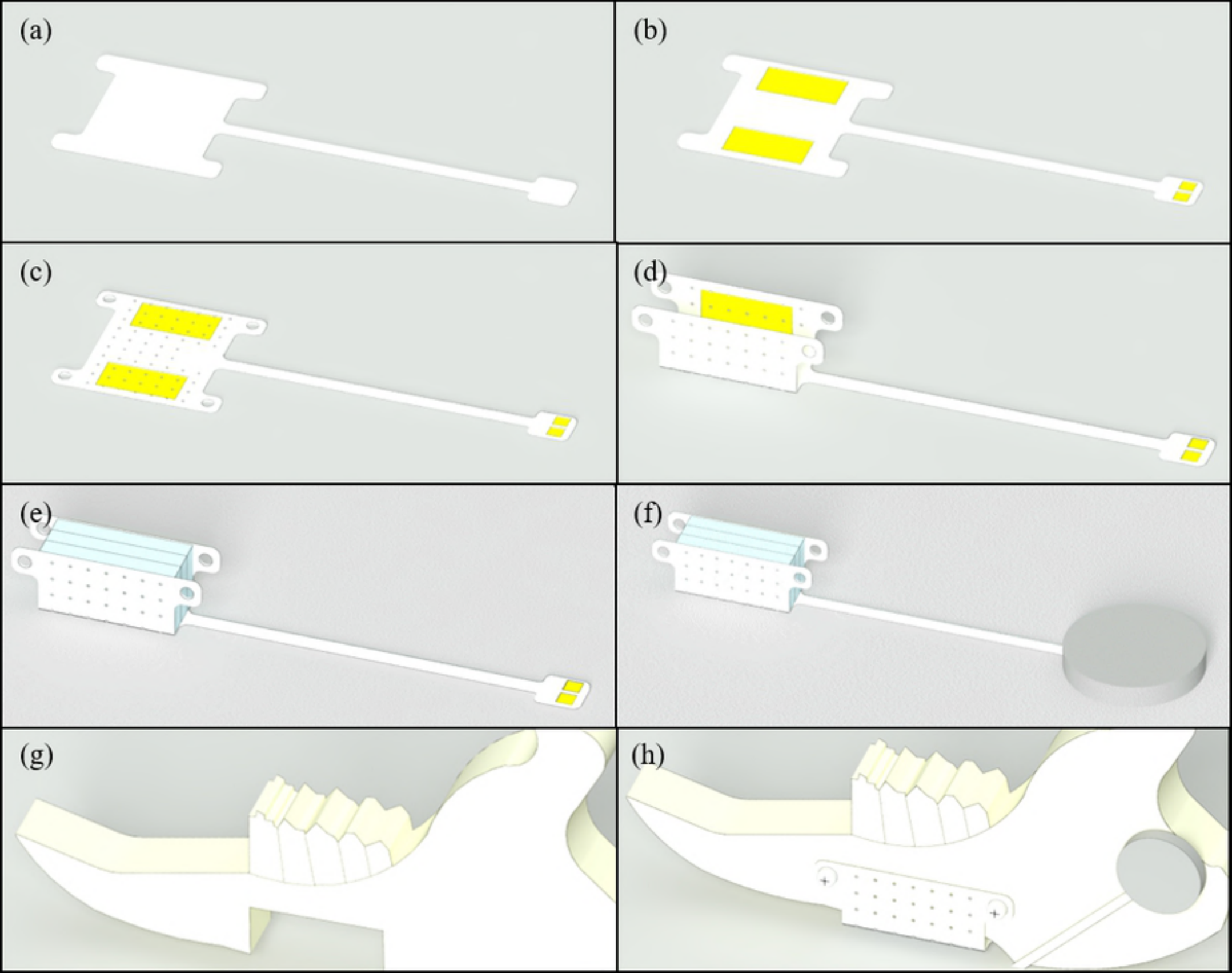
(a)
(b)
(c)
(d)
(e)
(f)
(g)
(h)